NANO LETTERS
Cite This: Nano Lett. 2018, 18, 1180−1184
Letter
pubs.acs.org/NanoLett

Reconfigurable Skyrmion Logic Gates

Shijiang Luo,[†] Min Song,[‡] Xin Li,[†] Yue Zhang,[†] Jeongmin Hong,[†] Xiaofei Yang,[†] Xuecheng Zou,[†] Nuo Xu,[§] and Long You*[,†]

[†]School of Optical and Electronic Information, Huazhong University of Science and Technology, Wuhan 430074, China
[‡]Faculty of Physics and Electronic Engineering, Hubei University, Wuhan 430062, China
[§]Department of Electrical Engineering and Computer Sciences, University of California, Berkeley, California 94720, United States

Supporting Information

ABSTRACT: Magnetic skyrmion, a nanosized spin texture with topological property, has become an area of significant interest due to the scientific insight that it can provide and also its potential impact on applications such as ultra-low-energy and ultra-high-density logic gates. In the quest for the reconfiguration of single logic device and the implementation of the complete logic functions, a novel reconfigurable skyrmion logic (RSL) is proposed and verified by micromagnetic simulations. Logic functions including AND, OR, NOT, NAND, NOR, XOR, and XNOR are implemented in the ferromagnetic (FM) nanotrack by virtue of various effects including spin orbit torque, skyrmion Hall effect, skyrmion−edge repulsions, and skyrmion−skyrmion collision. Different logic functions can be selected in an RSL by applying voltage to specific region(s) of the device, changing the local anisotropy energy of FM film. Material properties and geometrical scaling studies suggest RSL gates fit for energy-efficient computing as well as provide the guidelines for the design and optimization of this new logic family.

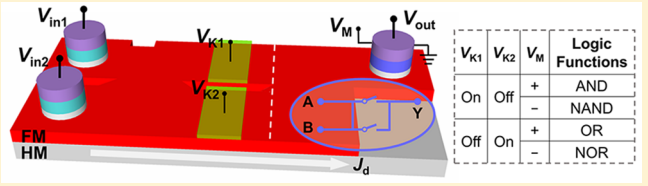

V_{K1}	V_{K2}	V_M	Logic Functions
On	Off	+	AND
		−	NAND
Off	On	+	OR
		−	NOR

KEYWORDS: *Skyrmion, logic gates, spintronic, magnetic tunnel junction, spin orbit torque, skyrmion Hall effect*

Magnetic skyrmions are considered as units (bits) in new magnetic data-storage devices, which are topological spin structure with whirling configuration generated at the ferromagnetic (FM) layer surface.[1−4] Due to their very small size (i.e., can be a few nanometers in diameter) and relatively low critical depinning current density (~10^6 A/m^2, defined as the minimum current density for a skyrmion to initiate its motion), there exists great potential for skyrmion-based magnetic memory and logic device applications,[5−8] in which skyrmions are regarded as the major carrier to transfer information, and binary data can be encoded with and without the presence of a skyrmion in an FM nanotrack. Skyrmion-based structures have advantages including topological stability, low operating power, and data nonvolatility realized in a small device footprint.

To allow varying operations to be performed efficiently with a minimal amount of devices, creating device that is adaptable for different logic functions or operations is an ingenious way to help design smaller, more-powerful, less-expensive, and more-reliable integrated circuit. Also, the completeness of Boolean operations is one of the essential tenets for logic implementation to enable feasible integrated circuit.[9] However, in the existing proposals of skyrmion-based logic,[10−12] the reconfiguration of single device and the implementation of the complete logic functions are lacked.

In this work, complete logic family including AND/OR/XOR and NOT/NAND/NOR/XNOR are implemented based on our skyrmion logic gates, in which the skyrmion's moving trajectories are manipulated by virtue of various effects including spin orbit torque (SOT),[13,14] skyrmion Hall effect (SkHE),[15−19] skyrmion-edge repulsions,[20,21] and the voltage control of magnetic anisotropy (VCMA) effect.[22,23] In addition, the proposed logic devices only utilize single skyrmion's motion and interaction between skyrmions in the FM film without the interactions between the skyrmion(s) and domain wall,[10−12] which, to the maximum extent, simplifies the design and operation of skyrmion-based devices. The aforementioned logic functions can be integrated on one single skyrmion device and reconfigured by controlling terminal voltages, which generates a new kind of logic gates to existing spintronic device family: the reconfigurable skyrmion logic (RSL) gates.

Simulation Methodology. Micromagnetic simulations using object-oriented micromagnetic framework (OOMMF) are performed to study the dynamical behaviors of skyrmions with the interfacial Dzyaloshinskii−Moriya interaction (DMI) effect[24] included. The adopted mesh size is 1 nm × 1 nm × 1 nm with one site in the thickness direction. A Co/Pt bilayer with perpendicular magnetization anisotropy (PMA) was used as the FM medium for skyrmions. The material-related parameters are as follows. The saturation magnetization (M_S), the exchange stiffness constant (A), the DMI constant (D), the PMA constant (K_u), the spin Hall angle (θ_{SH}), and the damping coefficient (α) are 5.8 × 10^5 A/m, 1.5 × 10^{-11} J/m, 3 mJ/m^2, 0.8 × 10^6 J/m^3, 0.08, and 0.3, respectively.

Received: November 8, 2017
Published: January 19, 2018

DOI: 10.1021/acs.nanolett.7b04722
Nano Lett. 2018, 18, 1180−1184

Table 1. Studied MTJ structures[a]

MTJ				
State	P	AP	Quasi-P	Quasi-AP
θ	0°	180°	37°	143°
TMR	0%	100%	10.6%	67.8%
R	LRS	HRS	LRS	HRS
Data	0	1	0	1
Sk	w/o	w/o	w/	w/

[a]Their corresponding states of two FM layers: parallel (P), antiparallel (AP), quasi-parallel (Quasi-P), and quasi-antiparallel (Quasi-AP); averaged angles (θ) of magnetization moments between two FM layers; tunnelling magnetoresistance (TMR) variation with respect to the case of $\theta = 0°$; resistance (R): low-resistance state (LRS), high-resistance state (HRS); binary data levels with (w/) and without (w/o) the presence of skyrmion (Sk) in an MTJ.

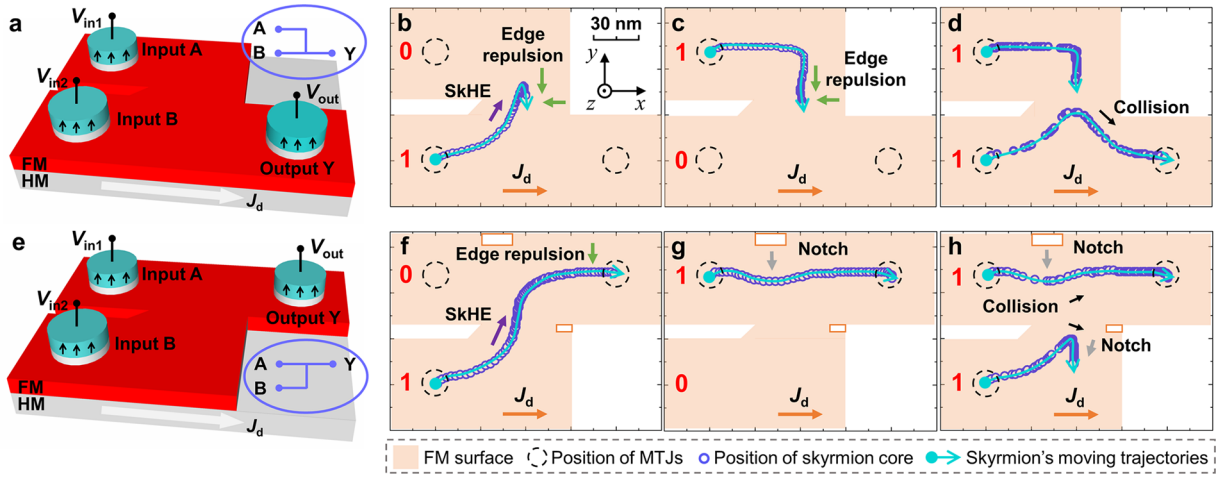

Figure 1. Skyrmion logic AND gate: (a) the device structure with two inputs and one output and (b–d) micromagnetic simulations of trajectories of skyrmion motion in FM films under three cases of inputs. Skyrmion logic OR gate: (e) the device structure with two inputs and one output and (f–h) micromagnetic simulations of trajectories of skyrmion motion in FM films under three cases of inputs.

The skyrmion can be considered as a rigid quasi-particle, which provides a great convenience for theoretical research of skyrmion dynamics.[25] A skyrmion can be generated by local injection of a spin-polarized current into FM layer surface[26] and then be driven by a current flowing in the heavy metal (HM) layer via SOT. The SOT-driven skyrmion's motion is modeled using the Thiele equation[25−28]

$$\vec{G} \times \vec{v} + \alpha \vec{\vec{D}} \cdot \vec{v} + \vec{F}_{spin} + \vec{F} = 0 \quad (1)$$

The first term on the left side represents the Magnus force[29] that gives rise to the SkHE (i.e., the skyrmion trajectories bend away from the direction of the conduction electron flow). G is the so-called gyrocoupling vector, and v is the drift velocity of the skyrmion. $\vec{\vec{D}}$ is the dissipative tensor. F_{spin} represents the SOT driving force by spin current generated by the spin Hall effect of the HM layer. F denotes to the resultant force acting on the skyrmion from FM track edges, defects, impurities, another skyrmions and so on when they approach to each other. Here, defects and impurities are not taken into account.

Skyrmion-Based Binary Data Representation. The mechanism to read out a skyrmion is through a magnetic tunnel junction (MTJ) structure. The bottom FM contacted with HM layer works as the free layer of the MTJ. The top FM layer acts as the fixed layer. The resistance of MTJ depends on the angle (θ) of the two FM layers' magnetization moments due to the tunnelling magnetoresistance (TMR) effect, which can be divided into two states, i.e., the high-resistance state (HRS) and the low-resistance state (LRS). Once the skyrmion appears in the free layer, the core of skyrmion is either in parallel with or antiparallel to the fixed layer, denoting as the quasi-parallel or quasi-antiparallel states. As expected, there exist four states in studied MTJ structures, namely, parallel (P), antiparallel (AP) (without a skyrmion), quasi-parallel (Quasi-P) and quasi-antiparallel (Quasi-AP) states (with a skyrmion), as shown in Table 1.

The resistance (R) of an MTJ can be expressed as[30]

$$R = \frac{2}{G_p + G_{ap} + (G_p - G_{ap})\cos\theta} \quad (2)$$

with G_p and G_{ap} representing the conductances of P ($\theta = 0°$) and AP ($\theta = 180°$) states, respectively. G_p is set to be twice of G_{ap}, corresponding to a peak TMR of 100%. The average θ between a skyrmion and the fixed layer in the MTJ region is calculated. The average θ for Quasi-P and Quasi-AP state is about 37° and 143°, and the TMR is 10.6% and 67.8%, respectively. The four MTJ states are classified as two binary

DOI: 10.1021/acs.nanolett.7b04722
Nano Lett. 2018, 18, 1180−1184

data levels. P and Quasi-P states are encoded as "0", while AP and Quasi-AP states are defined as "1".

Implementation of AND and OR Logic Functions. In the proposed structure shown in Figure 1a, two input-MTJs A and B are placed at the left side, while an output-MTJ Y is placed at the lower right side. It is noted that the magnetization is pointing up in fixed layer of MTJs so that state "0" corresponds to the absence of a skyrmion and "1" corresponds to the presence as mentioned above. When input voltage (V_{in}) is below the critical value (V_c) to overcome the topological stability barrier, no skyrmion appears in the free layer of the input-MTJ. At $V_{in} > V_c$, a sufficiently large spin-polarized current is applied to create a skyrmion. The created skyrmion then moves toward right under drive current (J_d). If a skyrmion reaches bottom layer of the output-MTJ, it results in a high-resistance state and consequently a high output voltage (V_{out}). If no skyrmion is detected by the output-MTJ, a low V_{out} is output.

When both inputs are "0" state ($V_{in} < V_c$), there are no skyrmions moving in the FM nanotrack. Figure 1b–d shows the trajectories of skyrmion motions in FM film under another three cases of inputs. As shown in Figure 1b, an individual skyrmion at lower left moves (about 60 nm) along the $+x$ direction due to SOT and simultaneously deviates to the $+y$ direction (for a distance about 50 nm) because of the SkHE. Then the skyrmion stops at the center region due to the repulsion from track edge. If a skyrmion starts to move from upper left, it moves along the edge of FM film and stops (after a 35 nm) traveling along the $-y$ direction, as suggested by Figure 1c. However, when both of the skyrmions from lower and upper left move in this structure, the bottom one can reach lower right once it collides with top one (Figure 1d). As a result, only when both inputs are "1" state ($V_{in} > V_c$) can a skyrmion reach the output region. The states of two inputs and their corresponding outputs implements the function of AND (see Table S1 for the truth table of skyrmion logic AND gate).

If the upper right region is set as output, the function OR can be implemented as depicted in Figure 1e. In this structure, the individual skyrmions from lower or upper left can reach the upper right under drive current (Figure 1f,g). When the two are moving simultaneously, the top skyrmion can reach the upper right, while the bottom one gets impeded by an artificial notch after its collision with the top one (Figure 1h). To ensure the collision occurring at the center region, another rectangular (or triangular) notch[26] is set at upper edge to adjust the trajectory of top skyrmion. Consequently, a skyrmion can reach the output region, provided that one of the inputs is "1" (see Table S2).

Implementation of NOT Logic Function. The logic NOT is implemented in a straightforward way by switching the magnetization of the fixed layer of output-MTJ, as shown in Figure 2a. The magnetization switching can be induced by an in-plane current via SOT with the assistance of the exchange bias from antiferromagnetic (AFM) top layer.[31] In other words, the magnetization direction of the fixed layer can be controlled by the in-plane current (or voltage V_M) polarity. In this regime, when no skyrmion is created in the FM nanotrack, input is "0" state and output is "1" state (Figure 2b). When a skyrmion is created (i.e., input is "1" state) and then reaches the output region, output is switched to "0" state (Figure 2c; see Table S3)

Similarly, the function of NAND and NOR can be achieved based on existing AND and OR solutions (see Figure S1). Besides, by connecting the output-end of two skyrmion logic

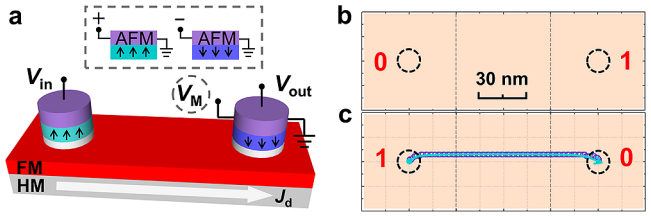

Figure 2. Skyrmion logic NOT gate. (a) The device structure with one input and one output. Inset: Polarity of control voltage V_M and corresponding magnetization direction. (b,c) A pair of cases of NOT operation and corresponding trajectories of skyrmion motion.

AND gates with the two input-ends of one skyrmion logic OR gate, it gives a way to the realization of logic XOR/XNOR (see Figure S2).

Reconfigurable Skyrmion Logic Gates. Furthermore, the logic function of AND and OR can be implemented in one structure by separating the outputs. Figure 3a–d shows the evolution of the position of skyrmion(s) under four cases of the inputs, respectively. According to the states of two inputs and their corresponding outputs, one can see that OR operation is executed at the upper right port, while AND operation is shown at the lower right.

Based on this structure, the reconfigurable skyrmion logic (RSL) gate structure is proposed to implement the aforementioned functions, as shown in Figure 3e. The function type can be selected by three voltage-control gates, where V_{K1} and V_{K2} are used to construct gates for controlling skyrmion motion via the modification of the anisotropy energy of local area in FM films under the applied voltage,[22] known as the VCMA effect.[23] When V_{K1}/V_{K2} is on, the K_u decreases in the controlled region, resulting in a repulsive dipolar forces acting on skyrmion so that its motion is impeded.[22] Therefore, when V_{K1} is on and V_{K2} is off, AND (NAND) operation is executed (see Figure S3); when V_{K1} is off and V_{K2} is on, OR (NOR) operation is executed (see Figure S4). Note that the stored data need to be erased by applying a pulsed drive current with large density for skyrmions' annihilation in the FM track before the next operation, denoted as the Erase operation.

RSL Gates Performance vs Scaling. The logic switching delay (t_d) is determined by the velocity (v) of skyrmion motion and the distance between input(s) and output. For one skyrmion logic unit, t_d is estimated to be around 10–20 ns at $J_d = 5 \times 10^{10}$ A/m^2 with $\theta_{SH} = 0.08$, which is comparable to that of current emerging nonvolatile switches based on spintronics and nanoelectro-mechanical technology.[9] Particularly, the skyrmion's velocity is proportional to J_d, as shown in Figure 4a. Thus, there exists a trade-off between delay t_d and the power consumption, and energy-efficient operations are optimal for RSL gates. Skyrmion's velocity is also affected by the magnetic properties of the FM film such as K_u and D. As shown in Figure 4b, the velocity increases as K_u decreases and D increases for a constant J_d. However, the skyrmion's size, governed by the diameter (d) of skyrmion in its steady state, is one of main factors to downscale the logic devices, which is further determined by magnetic properties such as K_u and D. As shown in Figure 4c, the diameter decreases as K_u increases and D decreases. Therefore, the switching delay is almost unaffected by scaling down the RSL gates via tuning magnetic properties including K_u and D.

In conclusion, functions including AND, OR, NOT, NAND, NOR, XOR, and XNOR are implemented in skyrmion logic

DOI: 10.1021/acs.nanolett.7b04722
Nano Lett. 2018, 18, 1180–1184

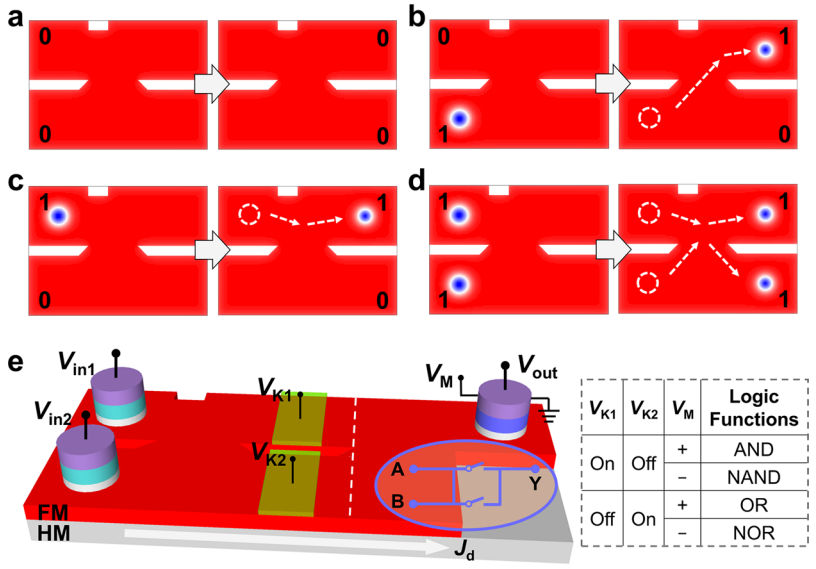

Figure 3. (a–d) Cases of inputs and their corresponding outputs and the evolution of the position of skyrmion(s) in FM films. (e) Structure of a reconfigurable skyrmion logic (RSL) gate, and configuration of three control voltages (V_{K1}, V_{K2}, and V_M) and the resulting logic functions in an RSL.

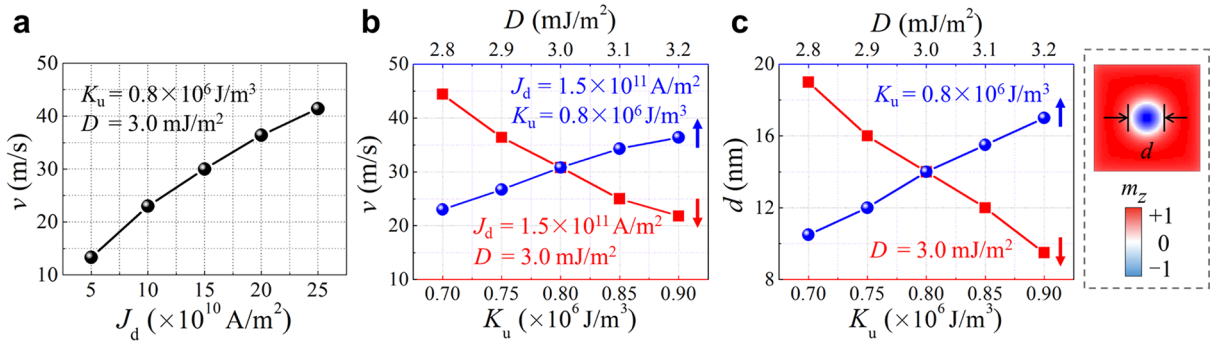

Figure 4. Skyrmion velocity (v) in steady motion as a function of (a) drive current density (J_d), (b) PMA constant (K_u), and DMI constant (D). (c) Skyrmion size (d), defined as the diameter of the circle within which $m_z = 0$, as a function of K_u and D.

gates, driven by current-induced SOT, SkHE, and skyrmion-edge repulsion effects. Within one device structure, different functions can be selected by additional voltage controls via the VCMA effect, enabling the reconfigurable logic styles. Material properties and geometrical scaling studies through micromagnetic simulations with predictive models suggest that reconfigurable skyrmion logic (RSL) is promising for nonvolatile and energy-efficient computing applications.

■ ASSOCIATED CONTENT

Supporting Information

The Supporting Information is available free of charge on the ACS Publications website at DOI: 10.1021/acs.nanolett.7b04722.

Truth tables of skyrmion logic AND, OR, and NOT gates; device structure of skyrmion logic NAND, NOR, and XOR/XNOR gates; and AND/NAND and OR/NOR operations of the reconfigurable skyrmion logic (RSL) gates. (PDF)

Movies for skyrmion motion in FM films under three cases of inputs of skyrmion logic AND, OR gates. (ZIP)

■ AUTHOR INFORMATION

Corresponding Author

*E-mail: lyou@hust.edu.cn.

Notes

The authors declare no competing financial interest.

■ ACKNOWLEDGMENTS

This work was supported by the National Natural Science Foundation of China (grant no. 61674062) and the Thousand Young Talents Program of China.

■ REFERENCES

(1) Mühlbauer, S.; Binz, B.; Jonietz, F.; Pfleiderer, C.; Rosch, A.; Neubauer, A.; Georgii, R.; Böni, P. Skyrmion Lattice in a Chiral Magnet. *Science* **2009**, *323*, 915–919.

(2) Yu, X. Z.; Onose, Y.; Kanazawa, N.; Park, J. H.; Han, J. H.; Matsui, Y.; Nagaosa, N.; Tokura, Y. Real-space observation of a two-dimensional skyrmion crystal. *Nature* **2010**, *465*, 901–904.

(3) Heinze, S.; von Bergmann, K.; Menzel, M.; Brede, J.; Kubetzka, A.; Wiesendanger, R.; Bihlmayer, G.; Blügel, S. Spontaneous atomic-scale magnetic skyrmion lattice in two dimensions. *Nat. Phys.* **2011**, *7*, 713–718.

(4) Yu, X. Z.; Kanazawa, N.; Onose, Y.; Kimoto, K.; Zhang, W. Z.; Ishiwata, S.; Matsui, Y.; Tokura, Y. Near room-temperature formation

DOI: 10.1021/acs.nanolett.7b04722
Nano Lett. 2018, 18, 1180–1184

of a skyrmion crystal in thin-films of the helimagnet FeGe. *Nat. Mater.* **2011**, *10*, 106−109.
(5) Kang, W.; Huang, Y.; Zhang, X.; Zhou, Y.; Zhao, W. Skyrmion-Electronics: An Overview and Outlook. *Proc. IEEE* **2016**, *104*, 2040−2061.
(6) Finocchio, G.; Büttner, F.; Tomasello, R.; Carpentieri, M.; Kläui, M. Magnetic skyrmions: from fundamental to applications. *J. Phys. D: Appl. Phys.* **2016**, *49*, 423001.
(7) Fert, A.; Cros, V.; Sampaio, J. Skyrmions on the track. *Nat. Nanotechnol.* **2013**, *8*, 152−156.
(8) Yu, G.; Upadhyaya, P.; Shao, Q.; Wu, H.; Yin, G.; Li, X.; He, C.; Jiang, W.; Han, X.; Amiri, P. K.; Wang, K. L. Room-Temperature Skyrmion Shift Device for Memory Application. *Nano Lett.* **2017**, *17*, 261−268.
(9) Nikonov, D. E.; Young, I. A. Overview of Beyond-CMOS Devices and a Uniform Methodology for Their Benchmarking. *Proc. IEEE* **2013**, *101*, 2498−2533.
(10) Zhang, X.; Ezawa, M.; Zhou, Y. Magnetic skyrmion logic gates: conversion, duplication and merging of skyrmions. *Sci. Rep.* **2015**, *5*, 9400.
(11) Xing, X.; Pong, P. W. T.; Zhou, Y. Skyrmion domain wall collision and domain wall-gated skyrmion logic. *Phys. Rev. B: Condens. Matter Mater. Phys.* **2016**, *94*, 054408.
(12) He, Z.; Angizi, S.; Fan, D. Current-Induced Dynamics of Multiple Skyrmions with Domain-Wall Pair and Skyrmion-Based Majority Gate Design. *IEEE Magn. Lett.* **2017**.8110.1109/LMAG.2017.2689721
(13) Jiang, W.; Upadhyaya, P.; Zhang, W.; Yu, G.; Jungfleisch, M. B.; Fradin, F. Y.; Pearson, J. E.; Tserkovnyak, Y.; Wang, K. L.; Heinonen, O.; te Velthuis, S. G. E.; Hoffmann, A. Blowing magnetic skyrmion bubbles. *Science* **2015**, *349*, 283−286.
(14) Yu, G.; Upadhyaya, P.; Li, X.; Li, W.; Kim, S. K.; Fan, Y.; Wong, K. L.; Tserkovnyak, Y.; Amiri, P. K.; Wang, K. L. Room-Temperature Creation and Spin-Orbit Torque Manipulation of Skyrmions in Thin Films with Engineered Asymmetry. *Nano Lett.* **2016**, *16*, 1981−1988.
(15) Jiang, W.; Zhang, X.; Yu, G.; Zhang, W.; Wang, X.; Jungfleisch, M. B.; Pearson, J. E.; Cheng, X.; Heinonen, O.; Wang, K. L.; Zhou, Y.; Hoffmann, A.; te Velthuis, S. G. E. Direct observation of the skyrmion Hall effect. *Nat. Phys.* **2017**, *13*, 162−169.
(16) Litzius, K.; Lemesh, I.; Krüger, B.; Bassirian, P.; Caretta, L.; Richter, K.; Büttner, F.; Sato, K.; Tretiakov, O. A.; Förster, J.; Reeve, R. M.; Weigand, M.; Bykova, I.; Stoll, H.; Schütz, G.; Beach, G. S. D.; Kläui, M. Skyrmion Hall effect revealed by direct time-resolved X-ray microscopy. *Nat. Phys.* **2017**, *13*, 170−175.
(17) Chen, G. Spin-orbitronics: Skyrmion Hall effect. *Nat. Phys.* **2017**, *13*, 112−113.
(18) Nagaosa, N.; Tokura, Y. Topological properties and dynamics of magnetic skyrmions. *Nat. Nanotechnol.* **2013**, *8*, 899−911.
(19) Zang, J.; Mostovoy, M.; Han, J. H.; Nagaosa, N. Dynamics of Skyrmion Crystals in Metallic Thin Films. *Phys. Rev. Lett.* **2011**, *107*, 136804.
(20) Iwasaki, J.; Mochizuki, M.; Nagaosa, N. Current-induced skyrmion dynamics in constricted geometries. *Nat. Nanotechnol.* **2013**, *8*, 742−747.
(21) Zhang, X.; Zhao, G. P.; Fangohr, H.; Liu, J. P.; Xia, W. X.; Xia, J.; Morvan, F. J. Skyrmion-skyrmion and skyrmion-edge repulsions in skyrmion-based racetrack memory. *Sci. Rep.* **2015**, *5*, 7643.
(22) Upadhyaya, P.; Yu, G.; Amiri, P. K.; Wang, K. L. Electric-field guiding of magnetic skyrmions. *Phys. Rev. B: Condens. Matter Mater. Phys.* **2015**, *92*, 134411.
(23) Maruyama, T.; Shiota, Y.; Nozaki, T.; Ohta, K.; Toda, N.; Mizuguchi, M.; Tulapurkar, A. A.; Shinjo, T.; Shiraishi, M.; Mizukami, S.; Ando, Y.; Suzuki, Y. Large voltage-induced magnetic anisotropy change in a few atomic layers of iron. *Nat. Nanotechnol.* **2009**, *4*, 158−161.
(24) Rohart, S.; Thiaville, A. Skyrmion confinement in ultrathin film nanostructures in the presence of Dzyaloshinskii-Moriya interaction. *Phys. Rev. B: Condens. Matter Mater. Phys.* **2013**, *88*, 184422.
(25) Lin, S.-Z.; Reichhardt, C.; Batista, C. D.; Saxena, A. Particle model for skyrmions in metallic chiral magnets: Dynamics, pinning, and creep. *Phys. Rev. B: Condens. Matter Mater. Phys.* **2013**, *87*, 214419.
(26) Sampaio, J.; Cros, V.; Rohart, S.; Thiaville, A.; Fert, A. Nucleation, stability and current-induced motion of isolated magnetic skyrmions in nanostructures. *Nat. Nanotechnol.* **2013**, *8*, 839−844.
(27) Zhang, Y.; Luo, S.; Yan, B.; Ou-Yang, J.; Yang, X.; Chen, S.; Zhu, B.; You, L. Magnetic skyrmions without the skyrmion Hall effect in a magnetic nanotrack with perpendicular anisotropy. *Nanoscale* **2017**, *9*, 10212−10218.
(28) Thiele, A. A. Steady-State Motion of Magnetic Domains. *Phys. Rev. Lett.* **1973**, *30*, 230−233.
(29) Stone, M. Magnus force on skyrmions in ferromagnets and quantum Hall systems. *Phys. Rev. B: Condens. Matter Mater. Phys.* **1996**, *53*, 16573−16578.
(30) Jaffrès, H.; Lacour, D.; Nguyen Van Dau, F.; Briatico, J.; Petroff, F.; Vaurès, A. Angular dependence of the tunnel magnetoresistance in transition-metal-based junctions. *Phys. Rev. B: Condens. Matter Mater. Phys.* **2001**, *64*, 064427.
(31) Fukami, S.; Zhang, C.; DuttaGupta, S.; Kurenkov, A.; Ohno, H. Magnetization switching by spin-orbit torque in an antiferromagnet-ferromagnet bilayer system. *Nat. Mater.* **2016**, *15*, 535−541.

DOI: 10.1021/acs.nanolett.7b04722
Nano Lett. 2018, 18, 1180−1184